AD-A147 897 SOME IMPORTANT PROBLEM IN UNSTEADY BOUNDARY LAYERS INCLUDING SEPARATION I.. (U) MCDONNELL DOUGLAS CORP LONG BEACH CA T CEBECI ET AL. APR 84 MDC-J2990 1/1

UNCLASSIFIED AFOSR-TR-84-1066 F49620-82-C-0055 F/G 20/4 NL

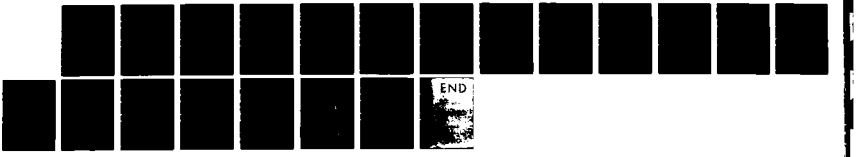

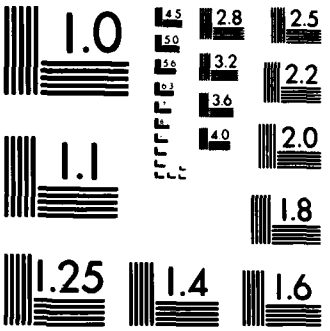

MICROCOPY RESOLUTION TEST CHART
NATIONAL BUREAU OF STANDARDS-1963-A

AFOSR-TR- 84-1066 Douglas Aircraft Report MDC J2990

SOME IMPORTANT PROBLEMS IN UNSTEADY BOUNDARY LAYERS INCLUDING SEPARATION

I. NATURE OF SINGULARITY ON OSCILLATING AIRFOILS

AD-A147 897

by

Tuncer Cebeci, A.A. Khattab and S.M. Schimke

April 1984

DTIC FILE COPY

Prepared under
Contract F49620-82-C-0055

for
Air Force Office of Scientific Research

DTIC ELECTE
1984

Approved for public release;
distribution unlimited.

84 11 26 114

UNCLASSIFIED
SECURITY CLASSIFICATION OF THIS PAGE

REPORT DOCUMENTATION PAGE

1a. REPORT SECURITY CLASSIFICATION Unclassified	1b. RESTRICTIVE MARKINGS
2a. SECURITY CLASSIFICATION AUTHORITY	3. DISTRIBUTION/AVAILABILITY OF REPORT Approved for Public Release; Distribution Unlimited.
2b. DECLASSIFICATION/DOWNGRADING SCHEDULE	
4. PERFORMING ORGANIZATION REPORT NUMBER(S)	5. MONITORING ORGANIZATION REPORT NUMBER(S) AFOSR-TR- 84-1066
6a. NAME OF PERFORMING ORGANIZATION DOUGLAS AIRCRAFT COMPANY 6b. OFFICE SYMBOL (If applicable)	7a. NAME OF MONITORING ORGANIZATION AFOSR/NA
6c. ADDRESS (City, State and ZIP Code) 3855 LAKEWOOD BOULEVARD LONG BEACH, CA 90846	7b. ADDRESS (City, State and ZIP Code) Bolling AFB, DC
8a. NAME OF FUNDING/SPONSORING ORGANIZATION AIR FORCE OFFICE OF SCIENTIFIC RESEARCH 8b. OFFICE SYMBOL (If applicable) AFSOR/NA	9. PROCUREMENT INSTRUMENT IDENTIFICATION NUMBER F49620-82-C-0055
8c. ADDRESS (City, State and ZIP Code) BOLLING AFB, DC 20332	10. SOURCE OF FUNDING NOS. PROGRAM ELEMENT NO. 61102F; PROJECT NO. 2307; TASK NO. A2; WORK UNIT NO
11. TITLE (Include Security Classification) SOME IMPORTANT PROBLEMS IN UNSTEADY BOUNDARY LAYERS INCLUDING SEPARATION (UNCLASSIFIED) I. NATURE OF SINGULARITY ON OSCILLATING AIRFOILS	
12. PERSONAL AUTHOR(S) TUNCER CEBECI A A KHATTAB S M SCHIMKE	
13a. TYPE OF REPORT ANNUAL 13b. TIME COVERED FROM _____ TO _____	14. DATE OF REPORT (Yr., Mo., Day) 1984, April 15. PAGE COUNT 18
16. SUPPLEMENTARY NOTATION	

17. COSATI CODES		
FIELD	GROUP	SUB. GR.

18. SUBJECT TERMS (Continue on reverse if necessary and identify by block number)
UNSTEADY VISCOUS FLOW
LAMINAR BOUNDARY LAYERS
SEPARATED FLOW
NUMERICAL MODELING

19. ABSTRACT (Continue on reverse if necessary and identify by block number)

Preliminary results are presented for the analysis of unsteady laminar boundary layers on oscillating airfoils. An examination of the evolution of the boundary layer near the nose of an oscillating airfoil has revealed that, when the reduced frequency is of the same order as in experiments on dynamic stall, the unsteady boundary layer ceases to behave in a smooth manner just downstream of separation and before one cycle is completed. As for the case of the impulsively started circular cylinder, the irregular behavior signals the onset of a singularity in the solution of the boundary layer equations. Numerical results for the method presented here are compared with the numerical results of van Dommelen and Shen for the impulsively started circular cylinder.

20. DISTRIBUTION/AVAILABILITY OF ABSTRACT UNCLASSIFIED/UNLIMITED ☒ SAME AS RPT. ☐ DTIC USERS ☐	21. ABSTRACT SECURITY CLASSIFICATION Unclassified
22a. NAME OF RESPONSIBLE INDIVIDUAL Major Michael S Francis	22b TELEPHONE NUMBER (Include Area Code) 202/767-4935 22c OFFICE SYMBOL AFOSR/NA

DD FORM 1473, 83 APR EDITION OF 1 JAN 73 IS OBSOLETE.

84 11 26 114

UNCLASSIFIED
SECURITY CLASSIFICATION OF THIS PAGE

1.0 INTRODUCTION

In recent years some important developments have occurred in the theory of two-dimensional laminar boundary-layer flows. The crucial discovery, due to van Dommelen and Shen[1], is that the solution of the boundary-layer equations with boundary conditions corresponding to a circular cylinder started impulsively from rest develops a singularity. This with u_∞ denoting the velocity of the cylinder and a its radius, occurs at a time $u_\infty t/a = 3.0$ and at an angular distance $\theta = 111°$ from the forward stagnation point. At this time the position of zero skin friction is at $\theta = 106°$ close to, but not coincident with, the singularity. This discovery was made by solving the governing boundary-layer equations in Lagrangian form; subsequently, the existence of the singularity was confirmed by Cebeci[2] using the Eulerian form and by Cowley[3] using the method of series truncation. The importance of this result is two-fold. First, it is of importance to the fundamental theory of high-Reynolds number flows in indicating that an interactive theory is necessary to understand the evolution of the flow field at a finite time after the motion starts, rather than only after a long time. Secondly, it is clear that significant changes will then occur in the flow field and these may be related to the phenomenon of vortex shedding. The physical processes which take place during the oscillation of the angle of attack of the airfoil are complicated and depend on a large number of parameters[4,5]. For example, an important characteristic is a large vortex that is formed near the surface at some stage in the cycle and causes stall to occur shortly afterwards. The occurrence of the vortex is probably associated with a breakdown of the unsteady boundary layer[6].

The purposes of the present research are to determine the relationship between unsteady separation and singularities in the solution, and to explore the possibilities of removing this singularity by interaction of the viscous and inviscid equations. In this report we describe the work that has been accomplished under the contract. So far we have examined the evolution of the boundary layer near the nose of an oscillating airfoil and found that, when the reduced frequency is of the same order as in the experiments on dynamic stall, the unsteady boundary layer ceases to behave in a smooth manner just downstream of separation and before one cycle has been completed; as with the impulsively started circular cylinder, this irregular behavior signals the onset of a singularity in the solution of the boundary-layer equations. The equations and

AIR FORCE OFFICE OF SCIENTIFIC RESEARCH (AFSC)
NOTICE OF TRANSMITTAL TO DTIC
This technical report has been reviewed and is approved for public release IAW AFR 190-12 (7b).
Distribution is unlimited.
MATTHEW J. KERPER
Chief, Technical Information Division

solution procedures used in the present study are described in Sections 2 and 3, respectively, and the results are presented and discussed in Section 4.

2.0 EQUATIONS, INITIAL AND BOUNDARY CONDITIONS

The boundary-layer equations and their boundary conditions for unsteady incompressible laminar flows on oscillating airfoils can be written as

$$\frac{\partial u}{\partial s} + \frac{\partial v}{\partial n} = 0 \tag{2.1}$$

$$\frac{\partial u}{\partial t} + u\frac{\partial u}{\partial s} + v\frac{\partial u}{\partial n} = \frac{\partial u_e}{\partial t} + u_e\frac{\partial u_e}{\partial s} + \nu\frac{\partial^2 u}{\partial n^2} \tag{2.2}$$

$$u(s,0,t) = 0,\ v(s,0,t) = 0,\ u(s,n_e,t) = u_e(s,t) \tag{2.3}$$

The solution of boundary-layer equations requires that the external velocity distribution be specified. Since the present effort is directed toward solutions near the leading edge of the airfoil, a local model for the potential flow has been chosen in the place of a full-potential-flow code. We consider an ellipse with major axis 2a and minor axis $2a\tau(\tau<<1)$ at an angle of attack $\alpha(t)$. The surface of the body is defined by

$$x = -a\cos\theta,\quad y = a\tau\sin\theta \qquad -\pi < \theta < \pi$$

and with these definitions and to a first approximation, the external velocity around the ellipse can be deduced from inviscid flow theory to be

$$u_e^o(s,t) = \frac{\xi + \xi_o}{\sqrt{1 + \xi^2}} \tag{2.4}$$

Here $\bar{u}_e^o(s,t)$ denotes a dimensionless velocity, $u_e^o/u_\infty(1 + \tau)$, the parameter ξ denotes a dimensionless distance related to the x- and y-coordinates of the ellipse by $x = 1/2\ a\tau^2\xi$, $y = a\tau^2\xi$ measured from the nose, and ξ_o $(\equiv\alpha/\tau)$ represents a dimensionless angle of attack. The parameter ξ is also related to the surface distance s by

$$s = a\tau^2 \int_0^\xi (1 + \xi^2)^{1/2} d\xi \tag{2.5}$$

We next define a dimensionless distance η by

$$\eta = \left[\frac{R(1+\tau)}{2\tau^2(1+\xi^2)}\right]^{1/2} \frac{n}{a} \tag{2.6a}$$

with $R = 2au_\infty/\nu$, and a dimensionless stream function f by

$$f(\xi,\eta,t) = [(1+\tau)au_\infty\nu\tau^2]^{-1/2}\psi(s,n,t) \tag{2.6b}$$

Introducing these relations together with Eq. (2.5) into Eqs. (2.1) and (2.2), it can be shown that the continuity and momentum equations can be written as

$$f''' + \frac{\xi}{1+\xi^2} f'^2 + (1+\xi^2)\bar{u}_e \frac{\partial \bar{u}_e}{\partial \xi} + (1+\xi^2)^{3/2} \frac{\partial \bar{u}_e}{\partial t_1} = f' \frac{\partial f'}{\partial \xi} - f'' \frac{\partial f}{\partial \xi}$$

$$+ (1+\xi^2) \frac{\partial f'}{\partial t_1} \tag{2.7}$$

Here primes denote differentiation with respect to η and $t_1 = (1+\tau)u_\infty t/a\tau^2$.

The boundary conditions for f and f' become

$$f = f' = 0 \quad \text{at} \quad \eta = 0,$$

$$f' \to (1+\xi^2)^{1/2} \bar{u}_e(\xi,t_1) \quad \text{as} \quad \eta \to \infty \tag{2.8}$$

The definition of $\bar{u}_e(\xi,t_1)$ is given by

$$\bar{u}_e(\xi,t) = \frac{u_e(\xi,t)}{u_\infty(1+\tau)} = \frac{\xi + \xi_0(t_1)}{\sqrt{1+\xi^2}} \tag{2.9}$$

To complete the formulation of the problem, initial conditions must be specified in the (t,n) plane at some $s = s_0$, either on the lower or upper surface of the airfoil as well as initial conditions in the plane on both surfaces of the airfoil. In the latter case, if we assume that steady-flow conditions prevail at $t = 0$, then the initial conditions in the (s,n)-plane can easily be generated for both surfaces by solving the governing equations for steady flow, which in this case, are given by Eq. (2.1) and by

$$u \frac{\partial u}{\partial s} + v \frac{\partial u}{\partial n} = u_e \frac{du_e}{ds} + \nu \frac{\partial^2 u}{\partial n^2} \tag{2.10}$$

There is no problem with the initial conditions for Eqs. (2.1) and (2.10) since the calculations start at the stagnation point.

The generation of the initial conditions in the (t,n)-plane are not so straightforward to obtain as is discussed in Section 3.1.

3.0 SOLUTION PROCEDURE

The solution procedure for the set of equations and boundary and initial conditions given in Section 2 can be achieved in two parts concerned, respectively, with the leading edge and downstream region. These two parts are considered in the following two subsections. In both cases the solution procedure makes use of Keller's box method, which is a two-point finite-difference scheme extensively used for the solution of parabolic partial-differential equations, as discussed by Bradshaw et al.[7].

3.1 Leading-Edge Region

The generation of the initial conditions in the (t,n)-plane at $s = s_0$ requires a special numerical procedure. Given, as we are, the complete velocity profile distribution on the previous time line, there is, in principle, no difficulty in computing values on the next time line by an explicit method, but if we wish to avoid the stability problems associated with such a method by using an implicit method, we are immediately faced with the problem of generating a starting profile on the new time line.

In order to explain the problem further, it is instructive to see what happens to the stagnation point as a function of time. For this purpose let us consider Eq. (2.4). If we choose $\xi_0(t_1)$ to be of the form $\xi_0(1 + A \sin\bar{\omega}t_1)$, and let $\bar{u}_e^0 \equiv u_e^0/u_\infty(1 + \tau)$, then Eq. (2.4) becomes

$$\bar{u}_e^0(\xi, t_1) = \frac{\xi + \xi_0(1 + A \sin\bar{\omega}t_1)}{\sqrt{1 + \xi^2}} \qquad (3.1)$$

where $\bar{\omega}$ is related to the dimensional frequency by

$$\bar{\omega} = \frac{a\tau^2}{(1 + \tau)u_\infty}\,\omega$$

Here ξ_0 and A denote parameters that need to be specified. Since by definition $\bar{u}_e^0 = 0$ at the stagnation point, its location, ξ_s, is given by

$$\xi_s = -\xi_0(1 + A \sin\bar{\omega}t_1) \tag{3.2}$$

and so the upper and lower surfaces of the airfoil as functions of time are defined, in particular, by $\xi > \xi_s$ and $\xi < \xi_s$. For example, let us take $A = 1$, $\omega = \pi/4$ and plot ξ_s/ξ_0 in the (t,ξ)-plane, as shown in Figure 1 for one cycle $(0 \leq t_1 \leq 8)$.

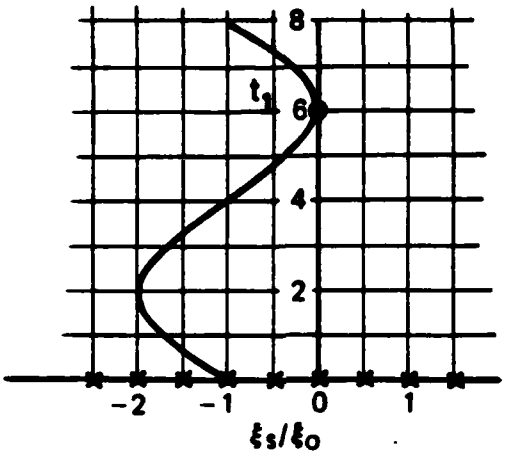

Fig. 1. Variation of stagnation point with time for one cycle according to Eq. (3.2), with $\bar{\omega} = \pi/4$, $A = 1$.

When $t_1 = 2$, the stagnation point ξ_s is at $-2\xi_0$, when $t_1 = 6$ is at 0, etc. If ξ_s were fixed, we could assume that $u = 0$ at $\xi = \xi_0$ for all time and all η, but this is not the case. It is also possible to assume that the stagnation point is coincident with zero u-velocity for a prescribed time. However, we should note that the stagnation point given by Eq. (3.2) is based on the vanishing of the external velocity. For a time-dependent flow, this does not necessarily imply that the u-velocity is zero across the layer for a given ξ-location and specified time. This point is substantiated by the results shown in Figure 2 taken from Ref. 8 and obtained with a novel numerical procedure called the characteristic box scheme. It is also evident from Figure 2 that flow reversals do occur due to the movement of the locus of zero u-velocity across the layer. This causes numerical instabilities which can be

avoided by using either the zig-zag box or the characteristic box finite-difference scheme. The details of these numerical schemes have been reported in Ref. 7 and, with special reference to oscillating airfoils, in Ref. 8.

3.2 Downstream Region

A solution to the leading-edge region, obtained by the procedure of Section 3.1, may be used as initial conditions for the solution of the system of equations given by Eqs. (2.7) and (2.8). This can conveniently be done by using Keller's box scheme, which reduces Eq. (2.7) to a first-order system. With f' and f" represented by r and v, respectively, we write

$$f' = r \tag{3.3a}$$

$$r' = v \tag{3.3b}$$

and obtain

$$v' + \frac{\xi}{1+\xi^2} r^2 + (1+\xi^2)\bar{u}_e \frac{\partial \bar{u}_e}{\partial \xi} + (1+\xi^2)^{3/2} \frac{\partial \bar{u}_e}{\partial t_1} = r \frac{\partial r}{\partial \xi} - v \frac{\partial f}{\partial \xi} + (1+\xi^2) \frac{\partial r}{\partial t_1} \tag{3.3c}$$

With this notation, the boundary conditions given by Eq. (2.8) can be written as

$$f = r = 0 \qquad \text{at} \quad \eta = 0 \tag{3.4}$$

$$r_e = (1+\xi^2)^{1/2}\bar{u}_e \qquad \text{at} \quad \eta = \eta_e \tag{3.5}$$

The system of Eqs. (3.3) and (3.4) has been solved by the numerical procedure of Ref. 7.

4.0 NATURE OF THE SINGULARITY FOR AN OSCILLATING AIRFOIL

One phase of the calculations for the oscillating airfoil was carried out by choosing $\xi_0 = 1$, $A = -1/2$ and $\bar{\omega} = 0.1$. With these choices the maximum value of α_{eff}, defined by

$$\alpha_{eff} = \xi_0(1 + A \sin\bar{\omega}t_1) \tag{4.1}$$

is sufficient to provoke separation with a strong singularity if the boundary layer were steady. At present ξ_0, A, $\bar{\omega}$ are being varied to examine their effect on the nature of singularity.

The unsteady flow calculations displayed in Fig. 3 show that the boundary layer eventually separates, the flow remaining smooth. However, just downstream of separation, it is evident that a singularity develops in the solution in the neighborhood of $\xi = 2.12$ and $\bar{\omega}t_1 = 308.75°$ and that it is not possible to continue the solution beyond this time without conceptual changes in the mathematical and physical formulation of the problem. While this is a satisfying conclusion, and may be interpreted as giving theoretical support to experimental observations of dynamic stall, it should be treated with some caution. Boundary-layer singularities have been the subject of much controversy in recent years and it is clearly important to make sure that any irregularities in a computed solution are not creatures of the numerical method used. We, however, feel confident that the calculations reported here are accurate and that the singularity is real.

Figure 3a shows that the variation of the displacement thickness

$$\gamma^* = \frac{\delta^*}{a}\left(\frac{1+\tau}{\tau}\right)\frac{1}{\varepsilon\pi} \tag{4.2}$$

is generally smooth except in the neighborhood of $\xi = 2.12$ and for $\bar{\omega}t_1 = 308.75°$. The first sign of irregularity is the steepening of the slope of γ^* when $\bar{\omega}t_1 = 300°$. A local maximum of γ^* occurs at $\xi = 2.12$ when $\bar{\omega}t_1 = 308.75°$. When the same results are plotted for a displacement velocity, $(d/d\xi)(u_e\delta^*)$, (Fig. 3b), we observe that the steepening of the displacement velocity near $\xi = 2.12$ is dramatic. For example, for $\bar{\omega}t_1 = 300°$, the peak is at $\xi = 2.125$, for $\bar{\omega}t_1 = 305°$, it is at $\xi = 2.105$, for $\bar{\omega}t_1 = 307.5°$, it is at $\xi = 2.09$ and finally for $\bar{\omega}t_1 = 308.75°$, the peak moves to $\xi = 2.08$. It should be noted that the maximum value of displacement velocity moves towards the separation point with increasing $\bar{\omega}t_1$; the same behavior will be shown to occur for the circular cylinder discussed below.

As shown in Fig. 3c, the wall shear parameter f''_w shows no signs of irregularity for $\bar{\omega}t_1 \leq 308.75°$ but a deep minimum in f''_w occurs near $\xi = 2.15$, i.e. near the peak of γ^*.

It is interesting and useful to compare the results presented in Fig. 3 for an oscillating airfoil with those obtained for a circular cylinder started impulsively from rest. This comparison lends support to the accuracy of the present calculation method and at the same time enables us to compare the characteristics of two distinctly different unsteady flows near the singularity location. The circular cylinder problem has been extensively studied as reported in Refs. 9 and 10 and the present results shown below are in close agreement with those of previous authors, but with subtle differences which may have important implications.

Figure 4 shows the results obtained by Cebeci[2] for the circular cylinder problem. As in the case of the oscillating airfoil, the flow separates and remains smooth up to the separation point. However, just downstream of separation with increasing time, a singularity develops in the neighborhood of $\theta = 112°$ and $t \approx 3.0$ and it was not possible to continue the boundary-layer calculations beyond this time and angular location. From Fig. 4a we see that while the variation of displacement thickness is smooth for values of θ less than 108°, it begins to steepen dramatically thereafter. The same results are plotted in Fig. 4b to demonstrate that, as in Fig. 3b, the displacement velocity exhibits a maximum which increases rapidly with time. Again the maximum shifts towards the location of separation with increasing time.

The results of local skin-friction coefficient calculations in Fig. 4c follow similar trends of those obtained for the oscillating airfoil. In both cases, the distributions pass through zero with no signs of irregularity and do not exhibit any breakdown before the time corresponding to the singularity.

The very careful calculations of van Dommelen and Shen are reproduced on Figures 5 and 6 for displacement thickness and velocity profiles, respectively. The corresponding displacement thickness results of Cebeci[2] together with the new calculations of the velocity profiles are reproduced for comparison purposes. As can be seen from Fig. 5, the agreement between the sets of calculations for three values of $t = 2$, 2.5 and 2.75 is excellent. The velocity

profiles of Fig. 6a, which correspond to a time t = 2.75 as in Fig. 5c, are also in excellent agreement for various angular locations. In contrast, the calculated velocity profiles of van Dommelen and Shen[11] at t = 2.984375 show differences from the present results obtained at t = 2.9875. The figure confirms the expected close agreement of the two sets of results at the two smallest angular locations, but indicates significant differences at the two highest values. The trend is different in that the present results show that the location and the magnitude of the maximum negative velocity increases with angular location. Also the tendency for flattening of the velocity profiles in the vicinity of the singularity is not confirmed by the present results.

Figure 7 shows the velocity profiles obtained by Cebeci[2] for two values of t as a function of angular location. It is clear that the magnitude of negative velocity increases with angular location and suggests that as the singularity is approached, the magnitude of the negative velocity will tend to infinity.

Figure 8 allows comparison of the displacement velocities obtained by Cowley[3] and by the present method for four values of time. We would expect, from the previous comparisons that the two sets of results would be in close accord at least for times up to 2.75. The figure shows the expected close agreement until the maximum value is approached. The discrepancies apparent at higher values of θ cannot readily be explained, and it should be noted that the location and time of singularity occur at different values of θ; the results of Cowley and van Dommelen and Shen appear to agree in this respect. The reasons for these discrepancies are presently under investigation.

5.0 REFERENCES

1. van Dommelen, L.L. and Shen, S.F.: The Genesis of Separation. In Numerical and Physical Aspects of Aerodynamic Flows (ed. T. Cebeci), Springer-Verlag, NY, 1982.

2. Cebeci, T.: Unsteady Separation. In Numerical and Physical Aspects of Aerodynamic Flows (ed. T. Cebeci), Springer-Verlag, NY, 1982.

3. Cowley, S.: Private communication.

4. McCroskey, W.J. and Pucci, S.L.: Viscous-Inviscid Interaction on Oscillating Airfoils in Subsonic Flow. AIAA J., 20, 167-174, 1982.

5. Carr, L.W., McCroskey, W.J., McAlister, K.W., Pucci, S.L. and Lambert, O.: An Experimental Study of Dynamic Stall on Advanced Airfoil Sections. Vol. 3. Hot-Wire and Hot-Film Measurements. NASA TM 84245, 1982.

6. Carr, L.W., McAlister, K.W. and McCroskey, W.J.: Analysis of the Development of Dynamic Stall Based on Oscillating Airfoil Experiments. NASA TN D-8382, 1977.

7. Bradshaw, P., Cebeci, T. and Whitelaw, J.H.: Engineering Calculation Methods for Turbulent Flows. Academic Press, London, 1981.

8. Cebeci, T. and Carr, L.W.: Prediction of Boundary-Layer Characteristics of an Oscillating Airfoil. In Unsteady Turbulent Shear Flows, Proc. Symp. (ed. R. Michel, J. Cousteix and R. Houdeville), Toulouse, France, 1981.

9. Cebeci, T. (ed.): Singularities in Unsteady Boundary Layers. In Numerical and Physical Aspects of Aerodynamic Flows, SpringerVerlag, NY, 1982.

10. Smith, F.T.: On the High Reynolds Number Theory of Laminar Flows. IMA J. Appl. Mech. 28, 207-281, 1982.

11. van Dommelen, L.L and Shen, S.F.: Private communication.

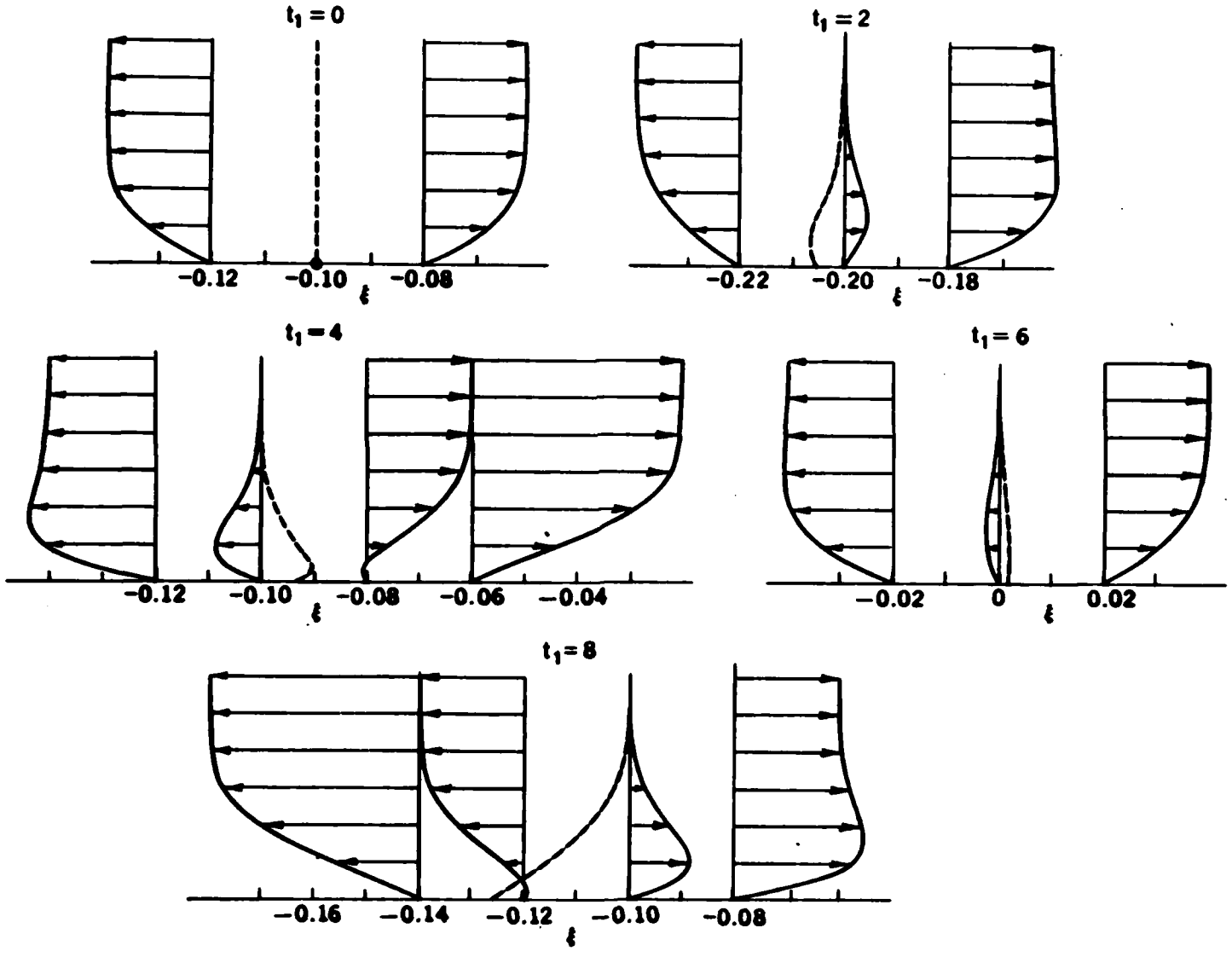

Fig. 2. Velocity profiles in the immediate neighborhood of the stagnation line at different times for $\omega = \pi/4$ and $A = 1$. The dashed lines indicate the locus of zero u-velocity across the layer.

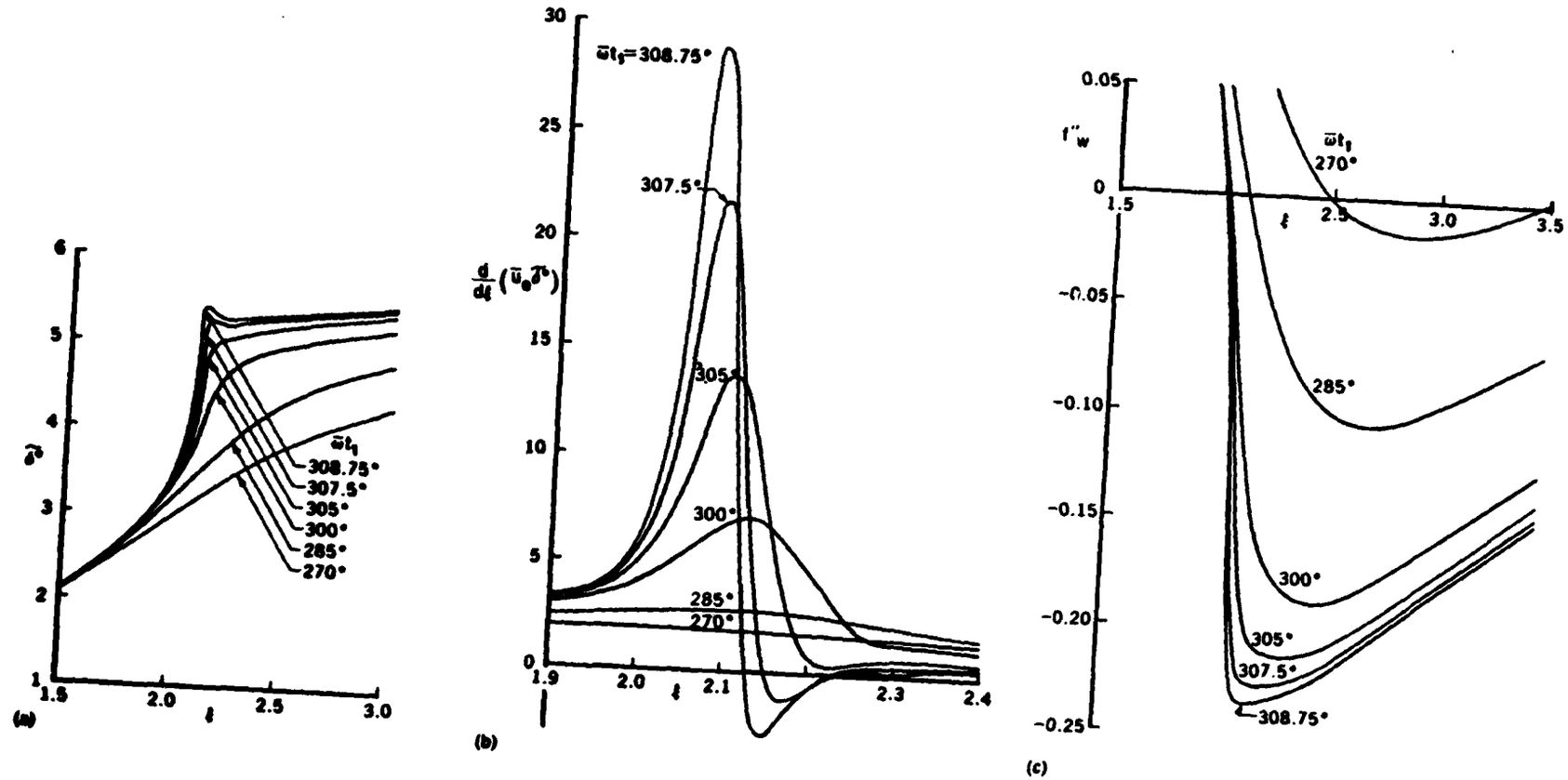

Fig. 3. Computed results for the oscillating airfoil, $A = -1/2$, $\bar{\omega} = 0.1$. (a) Displacement thickness $\tilde{\delta}^*$. (b) Displacement velocity, $d/d\xi\ (u_e\tilde{\delta}^*)$. (c) Wall shear parameter, f''_w.

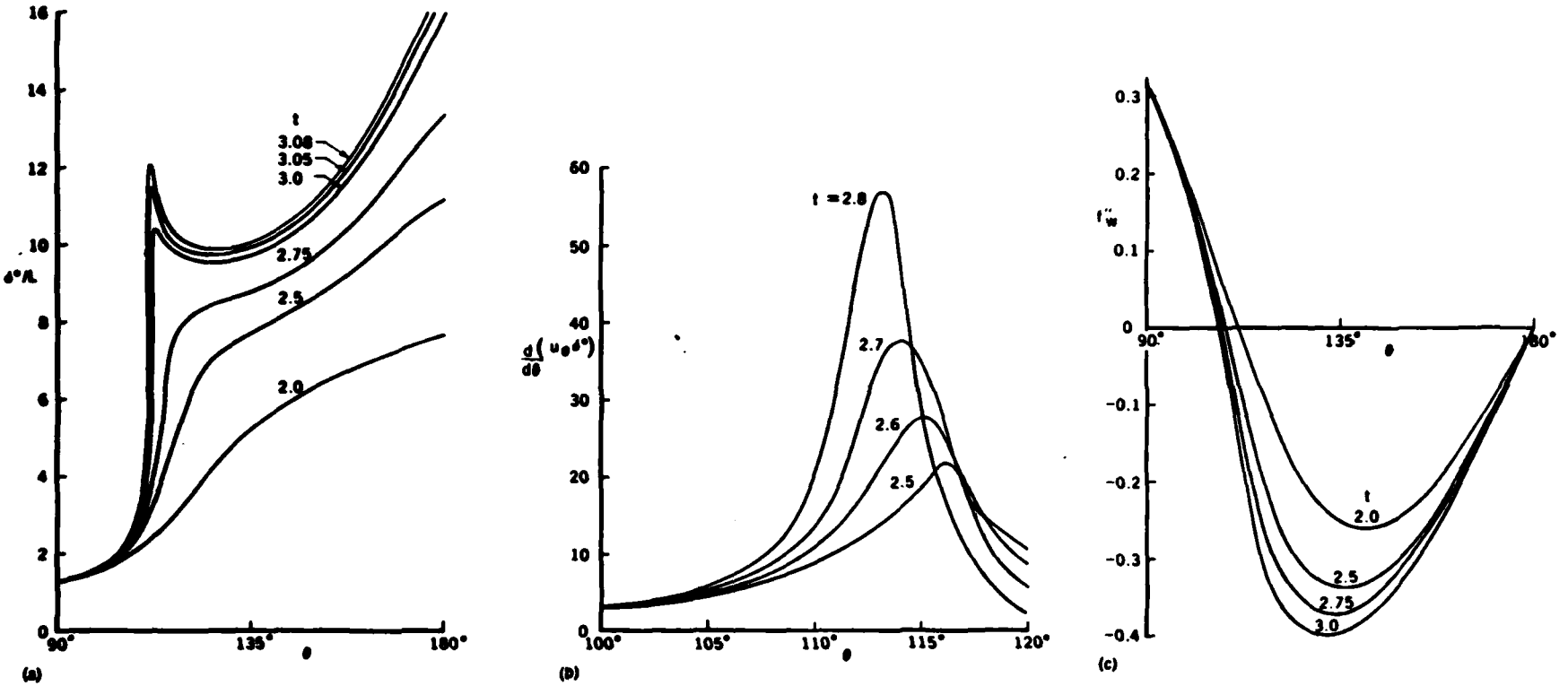

Fig. 4. Computed results of Cebeci[2] for the circular cylinder. (a) Displacement thickness δ^*/L. (b) Displacement velocity, $d/d\theta(u_e\delta^*)$. (c) Wall shear parameter, f''_w.

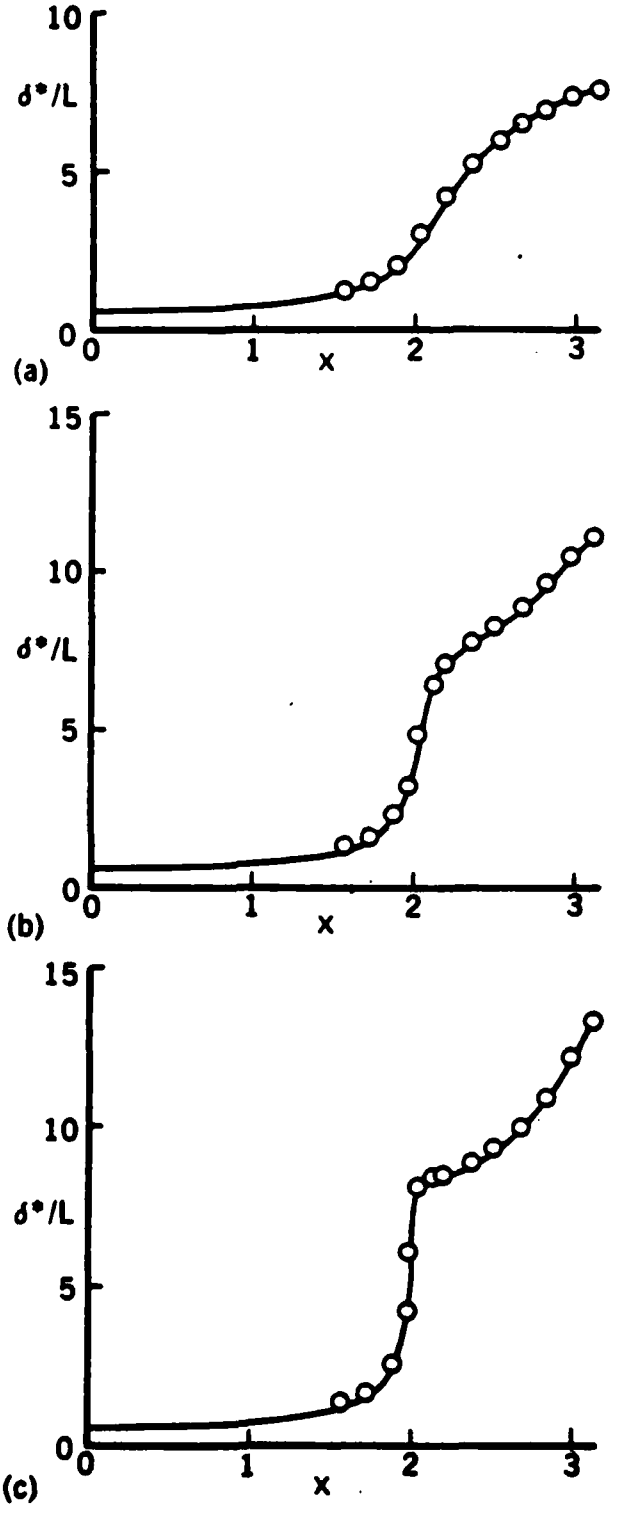

Fig. 5. Comparison between the displacement thickness values obtained by van Dommelen and Shen[1] (circles) and by Cebeci[2] (solid line) for the circular cylinder. (a) t = 2.0, (b) t = 2.5, (c) t = 2.75. (x is in radians.)

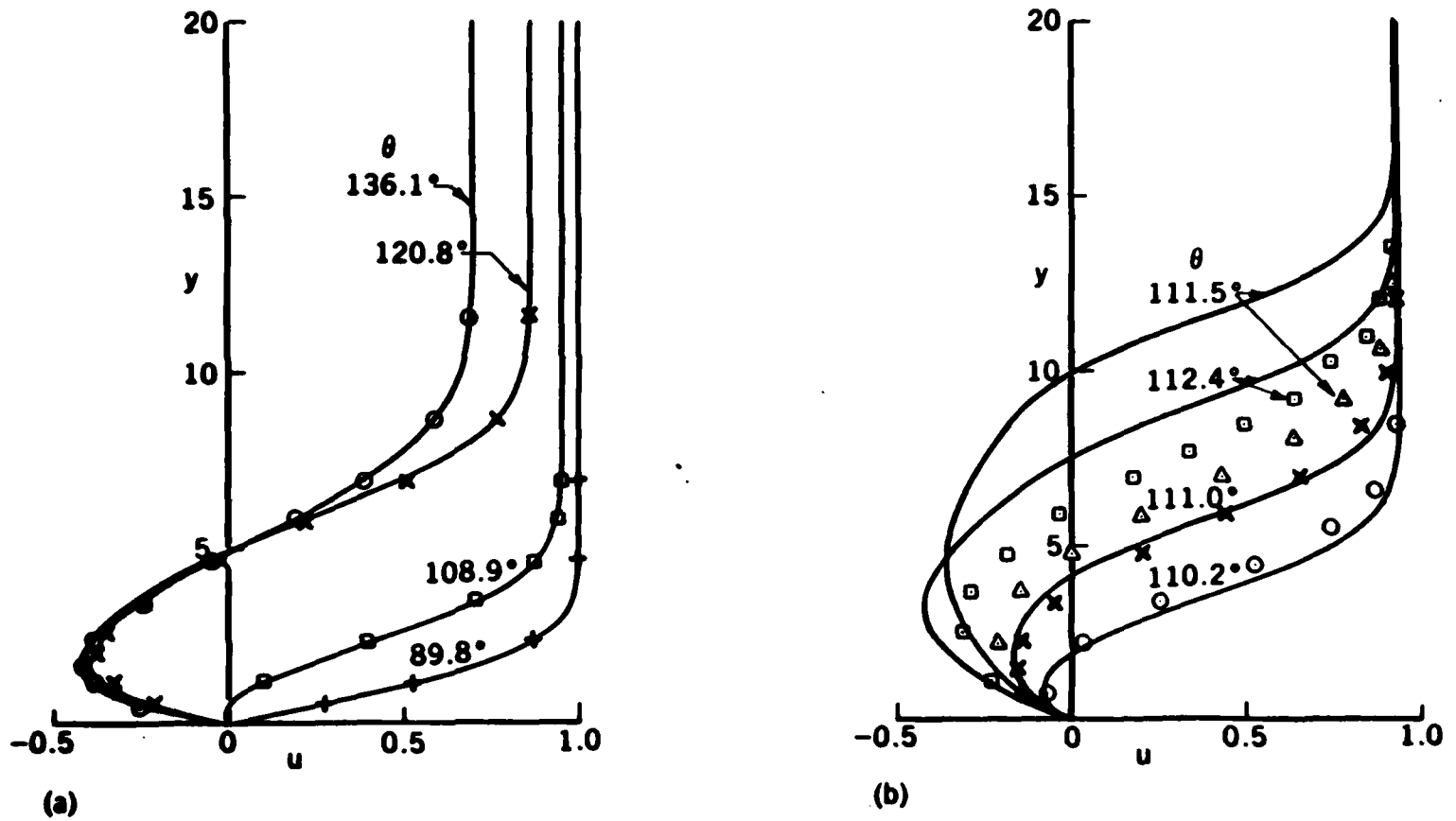

Fig. 6. Comparison between the velocity profiles obtained by van Dommelen and Shen[11] (solid lines) and by Cebeci[2] (symbols). (a) t = 2.75, (b) t = 2.984375 (van Dommelen and Shen) and t = 2.9875 (present calculations).

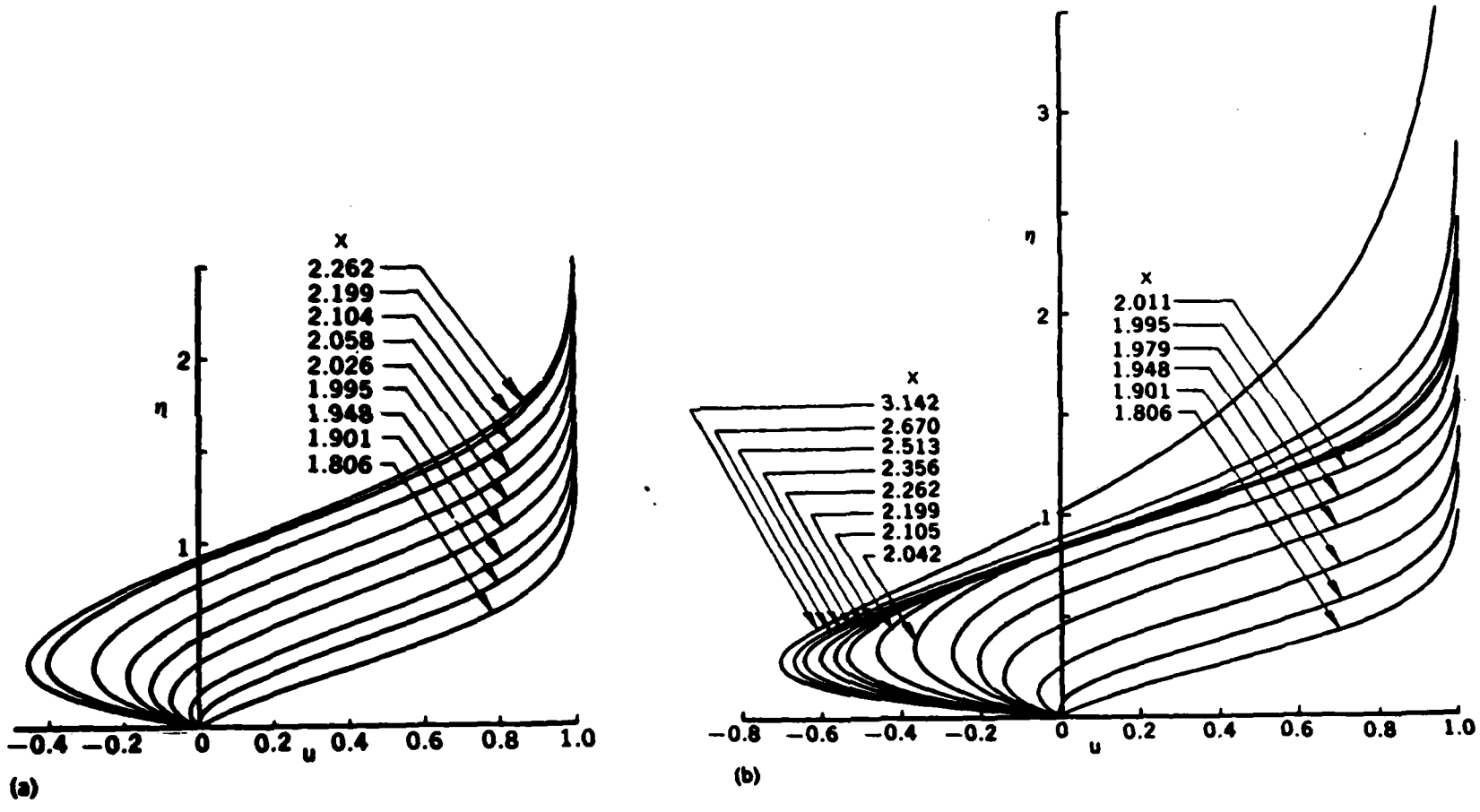

Fig. 7. Computed velocity profiles for the circular cylinder according to the calculations of Cebeci[2]. (a) t = 2.5, (b) t = 2.75. (x is in radians.)

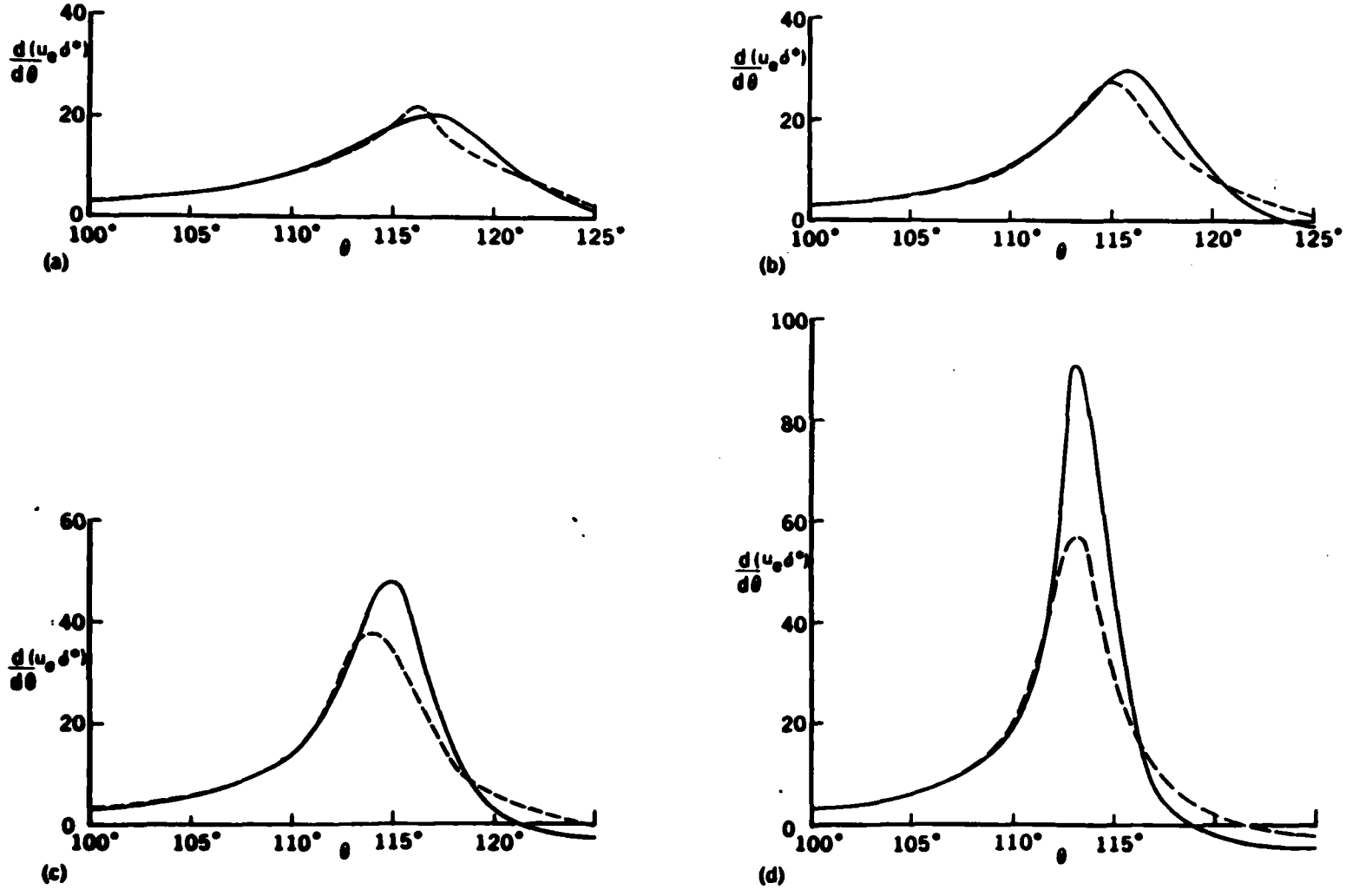

Fig. 8. Comparison between the displacement velocity values obtained by Cowley[3] (solid lines) and by the present method (dashed lines) for the circular cylinder. (a) t = 2.5, (b) t = 2.6, (c) t = 2.7, (d) t = 2.8.

END

FILMED

12-84

DTIC